Received: 5 June 2017 | Revised: 30 October 2017

DOI: 10.1002/hc.21406

RESEARCH ARTICLE

WILEY Heteroatom Chemistry

Improved complexation of paraquats with crown ether-based pyridyl cryptands

Terry L. Price Jr. | **Carla Slebodnick** | **Harry W. Gibson**

Department of Chemistry, Virginia Tech, Blacksburg, VA, USA

Correspondence
Harry W. Gibson, Department of Chemistry, Virginia Tech, Blacksburg, VA, USA.
Email: hwgibson@vt.edu

Funding information
National Science Foundation of the USA, Grant/Award Number: DMR 0704076, CHE-1106899, CHE-1507553

Abstract

The commonly used paraquat guest *N*,*N*′-dimethyl-4,4′-bipyridinium bis(hexafluorophosphate) (**7**) was targeted for structural alterations to improve the binding constants with crown ethers and cryptands. The association constant was improved by one order of magnitude (to $K_a = 1.00 \times 10^6$ mol L^{-1}) with the dibenzo-30-crown-10 pyridyl cryptand host **5** by changing the N-methyl groups to benzyl and the counterions from PF_6 to TFSI, that is, **11**. Moreover, through addition of a *p*-bromobenzyloxy moiety on the 4-position of the pyridyl ring of cryptand **18**, an association constant of $K_a = 5.35 \times 10^6$ mol L^{-1} was achieved with paraquat **11**.

1 | INTRODUCTION

In supramolecular chemistry, one of the most important parameters of a host-guest system is its association constant. By defining how well a host-guest pair bind one another, the experimentalist can determine what tasks may be achieved with the system. An example of this is the production of supramolecular polymers whose theoretical degree of polymerization (DP) may be calculated from the experimentally determined association constant (Equation 1), K_a, and $[H]_o$, the concentration of a heteroditopic (AB) monomer; clearly, higher association constants lead to higher DPs.[1]

$$\mathrm{DP} = \frac{2K_a[H]_o}{(1+4K_a[H]_o)^{1/2}-1} \quad (1)$$

if $4\,K_a[H]_o \gg 1$ then $\mathrm{DP} = (K_a\,[H]_o)^{1/2}$.

Our group focused on the evolution of dibenzo crown ether-based hosts to bind paraquat (*N*,*N*″-dialkyl-4,4′-bipyridinium salt) guests more strongly. Figure 1 and Table 1 show association constants reported by the Gibson and Huang groups. Through analysis of CPK models and crystal structures, host molecules have been advanced to highly evolved crown-based pyridyl cryptands, for example **5** and **6**. However, little improvement has been offered in way of the paraquat guest, the standard being dimethyl paraquat as the PF_6 salt (**7**) which displays reasonable association constants with various crown ethers[2–5] and analogous cryptands.[4,6–11]

Here, we investigate how alterations to the paraquat salt affect association constants with cryptands **5** and **6** as well as how accessing a less polar solvent can increase the association constant. Alterations to the paraquat salt were investigated in terms of the N-alkyl group and the counter anion. Focus was directed toward the association constants of cryptand **5**, given that its precursor crown ether **2** is produced through a high yielding templation process called the WPW process after its three key developers (Wang, Pederson, Wessels).[6,11–13] And diol **2** is converted to cryptand **5** in 89% yield via a template process.[14]

2 | RESULTS AND DISCUSSION

Given that the association constants for this study were expected to be relatively high, in excess of 1×10^4, ITC was used for their estimation. However, as the literature-reported values for **5•7** were obtained through ITC and **6•7** via an NMR study, the ITC titrations of **5•7** and **6•7** were carried out. Under similar ITC titration conditions (acetone, 23°C), the K_a of **5•7** was 2.21×10^5 mol L^{-1}, while that of **6•7** was 1.12×10^6 mol L^{-1}, bringing the separation of the values for the two cryptands to just under one order of magnitude. Note that the bis(*m*-phenylene)-32-crown-10-based pyridyl

Contract grant sponsor: National Science Foundation.

Contract grant number: DMR 0704076, CHE-1106899, CHE-1507553.

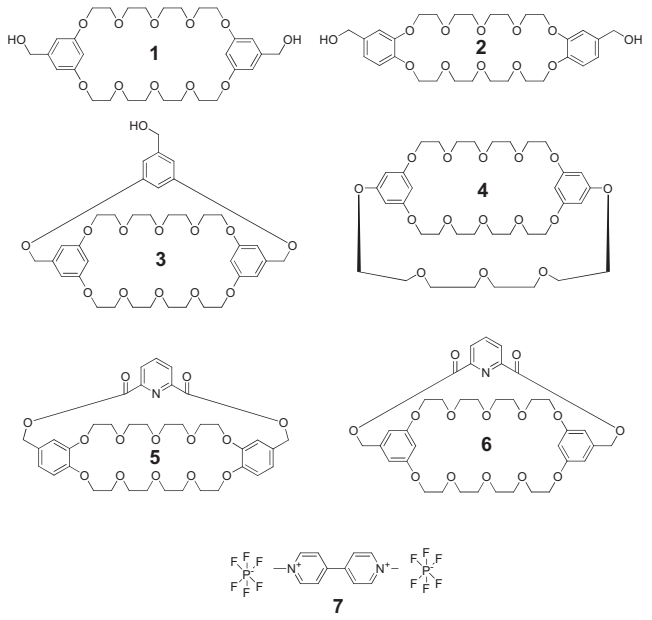

FIGURE 1 Various hosts investigated by the Gibson and Huang groups with dimethyl paraquat PF_6 (**7**)

TABLE 1 Association constants of hosts **1**-**6** with **7** in acetone at room temperature

Complex	K_a (mol L^{-1})
1•7[4b]	5.7×10^2
2•7[2]	1.1×10^3
3•7[7]	6.4×10^3
4•7[9]	6.1×10^4
5•7 (ITC)[6]	1.0×10^5
6•7 (NMR)[7]	5.0×10^6

cryptand **6** suffers from a low cyclization yield to form the precursor diol (cyclization yield to diester 43%),[15] while a very high yielding, template synthesis provides the analogous precursor to cryptand **5** in very high yield (cyclization yield to diester 93%).[6]

Table 2 provides a listing of paraquat guests investigated. Considering that solvents with higher dielectric constants lead to lower association constants, the paraquat salt design was focused toward solubility in relatively nonpolar solvents such as dichloromethane (DCM). Additionally, hosts such as **1**-**6** have low solubilities in solvents such as acetone. Salt solubilities are highly influenced by anion/cation combination, and paraquat salts such as **7** are typically soluble only in relatively polar aprotic solvents such as acetone. Changes in anion and increasing the organic character of the cation took priority. The bis(trifluoromethylsulfonyl)imide (TFSI) anion and large borate-based counterions have been well documented in the literature to increase the solubility of organic salts in low dielectric solvents because they are less ion paired than halides or PF_6^-,[16,17] consequently the TFSI and tetrakis(perfluorophenyl)borate anions were chosen for investigation. Regarding changes to the N-substituted group, the choice of benzyl in **10**-**13** was made because a wide range of benzyl building blocks is commercially available.

Table 3 lists the solubilities of paraquats **7**-**13** in acetone and DCM. Due to the high costs associated with tetrakis(perfluorophenyl)borate anion, only small amounts of **9** and **12** were synthesized, and no acetone solubility testing was conducted. A gain in acetone solubility of 13-fold was seen by simply going from PF_6 to TFSI counterions, **7** vs **8**. Similarly, by changing from an N-methyl to an N-benzyl group, a solubility increase of >4-fold was observed, **7** vs **10**. In terms of DCM solubility **9**, **11**, and **12** dissolved in DCM in measurable amounts, while **8** was only very, very sparingly soluble. Unfortunately perflurorobenzyl salt **13** was insoluble in DCM.

Table 4 compares association constants for the various host-guest pairs in acetone and DCM. Additionally, thermodynamic values are given for each titration. The first noticeable items in Table 4 are the deviations of **5•7** and **6•7** from the literature values. It is suspected that the deviation of **5•7** is a result of differences in data gathering. The reported K_a value of **5•7** was derived from a 33-point titration,[6] while values reported here were obtained using a 60-point titration curve; as the isotherm is fit to a mathematical construct, a more defined curve produces a better fit. As for the deviation of **6•7** from the literature values, this is attributed to differences in experimental methodologies; the reported value for **6•7** was obtained from a competitive NMR study,[7] while the results reported here within were obtained via ITC.

As seen in Table 4, improvements for host **5** were incremental with **8**, **10**, and **11** vs **7**, and **5•7** in acetone at 25°C has an association constant of 2.21×10^5 mol L^{-1}; however, changing PF_6 to TFSI, the N-methyl to N-benzyl, and by altering the titration solvent to DCM resulted in an improvement in K_a of **5•11** to 1.00×10^6 mol L^{-1}. Teasing out the effect of each change, we can see the effects of switching from acetone to DCM by looking at **5•11** in Table 4 for acetone and DCM. K_a did not change within experimental error, and ΔH and ΔS also remained the same within experimental error. As for the effects of changing to N-benzyl groups, we see in the titration of **5•8** compared to **5•11**, K_a increased 2.9-fold. In terms of ΔH and ΔS, the benzyl group leads to a more favorable enthalpy term that offsets a less favorable entropy term. The change in ΔH for **5•8** compared to **5•11**, −14.7 vs −18.1 kcal/mol, is likely attributable to the increased positive character of the N-benzylic protons relative to the N-methyl protons.

In comparison with PF_6, TFSI counterions consistently yielded higher association constants in complexes with

TABLE 2 Paraquat salts examined in this study

Counterion	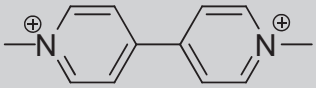	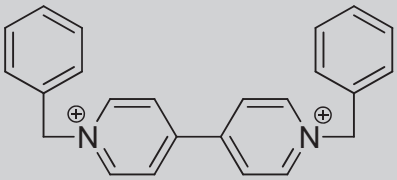
PF_6^-	**7**	**10**
$(CF_3SO_2)_2N^-$	**8**	**11**
$(C_6F_5)_4B^-$	**9**	**12**

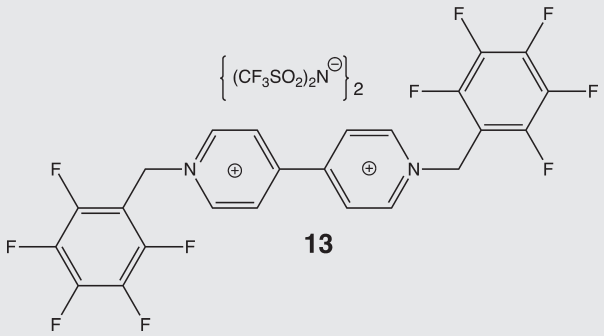

TABLE 3 Solubilities (mmol L^{-1}) of paraquats **7**-**13**

Compound	Acetone	DCM
7	56.2	Unobservable
8	749	<0.04
9	Not taken	0.49
10	261	Unobservable
11	1.08×10^3	6.26
12	Not taken	3.60
13	Not taken	Unobservable

5 (Table 4). Dimethyl paraquat displayed a 32% boost in its association constant by switching from PF_6 (in **5•7**) to TFSI (in **5•8**), while dibenzyl paraquat enjoyed a 28% increase (**5•10** vs **5•11**). In various other paraquat PF_6 (**7** and vinylogs) complexes with **5** and similar cryptands, the paraquat dication sits directly in the cavity of the cryptand nearly orthogonal to the pyridyl arm and does not penetrate the space between the two ethyleneoxy segments.[6,10,18,19] In a direct comparison of crystal structures of **5•7**[6] to **5•8**, there are several notable differences. First, in **5•8** (Figure 2), instead of sitting between the pyridyl arm and crown ether portion of the cryptand, the paraquat has inserted itself in such a way that one methyl group lies directly inside the crown ether segment of the ring. This new orientation leads to five hydrogen bonds at less than 3 Å with that methyl group; additionally, two protons on the paraquat ring provide four interactions that are less than

TABLE 4 ITC results for cryptands **5** and **6** with paraquats **7**, **8**, **10**, and **11**

	Solvent	K_a (mol L^{-1})	ΔG (kcal/mol)	ΔH (kcal/mol)	ΔS (cal/mol K)
5•7 (lit.)[6]	Acetone	1.00×10^5	−6.82	−13.0	−20.7
5•7	Acetone	2.21×10^5 ($\pm 0.22 \times 10^5$)	−7.29 (±0.73)	−14.8 (±0.2)	−25.3 (±2.5)
5•8	Acetone	2.86×10^5 ($\pm 0.17 \times 10^5$)	−7.44 (±0.44)	−14.7 (±0.1)	−24.2 (±1.5)
5•10	Acetone	6.49×10^5 ($\pm 0.54 \times 10^5$)	−7.93 (±0.66)	−18.9 (±0.1)	−36.7 (±3.1)
5•11	Acetone	8.34×10^5 ($\pm 0.49 \times 10^5$)	−8.08 (±0.48)	−18.1 (±0.1)	−33.7 (±2.0)
5•11	DCM	1.00×10^6 ($\pm 0.13 \times 10^6$)	−8.18 (±1.06)	−18.1 (±0.2)	−33.3 (±4.3)
5•13	Acetone	8.47×10^4 ($\pm 0.39 \times 10^4$)	−6.72 (±0.31)	−12.9 (±0.2)	−20.7 (±1.0)
6•7 (lit. via NMR)[7]	Acetone	5.0×10^6	N/A	N/A	N/A
6•7	Acetone	1.12×10^6 ($\pm 0.21 \times 10^6$)	−8.25 (±1.55)	−18.8 (±0.4)	−35.4 (±6.7)
6•8	Acetone	2.22×10^6 ($\pm 0.36 \times 10^6$)	−8.66 (±1.40)	−17.5 (±0.2)	−29.7 (±4.8)
6•11	DCM	1.41×10^6 ($\pm 0.23 \times 10^6$)	−8.39 (±1.37)	−13.8 (±0.1)	−18.2 (±3.0)

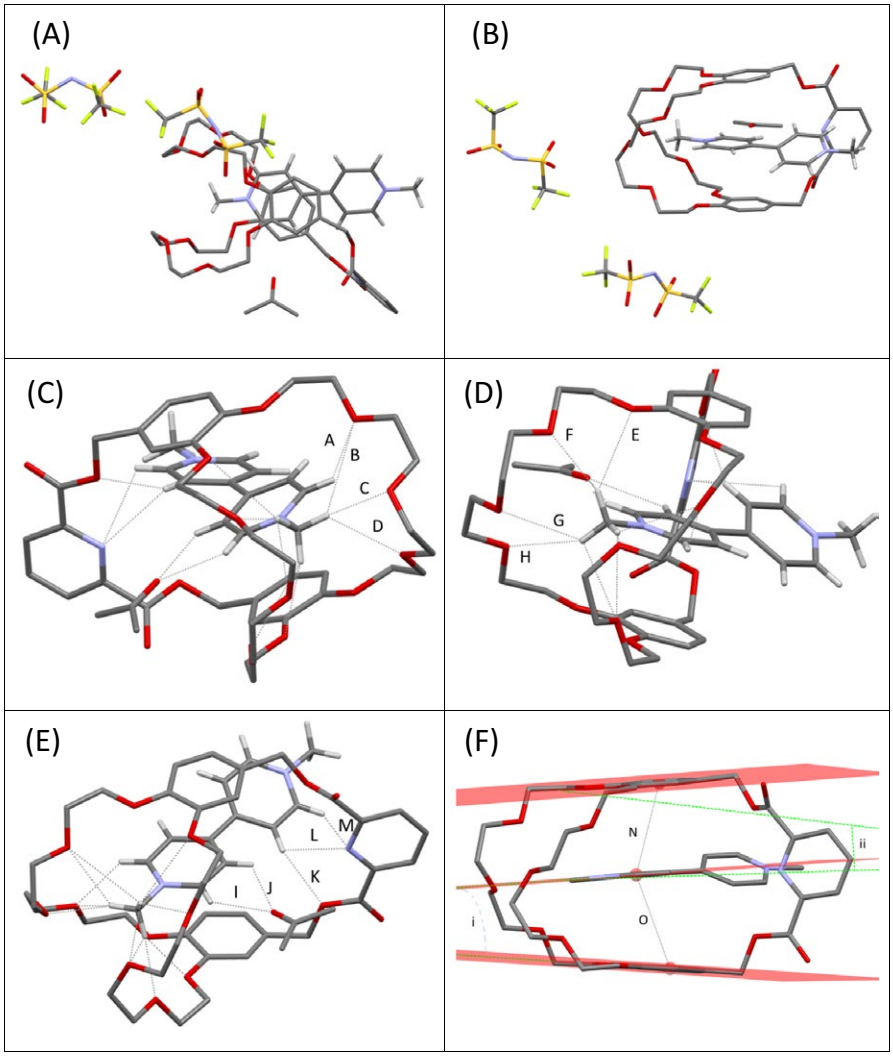

FIGURE 2 Crystal structure of **5•8** grown from a chloroform:acetone 1:1 (v:v) mixture by liquid-liquid diffusion of diethyl ether; nonparaquat hydrogen atoms and impurities have been removed for clarity; A, top view; B, side view; C, hydrogen bonding to the *p*-ethyleneoxy chain (counterions removed for clarity); D, hydrogen bonding to the *m*-ethyleneoxy chain (counterions removed for clarity); E, hydrogen bonding to acetone (solvent), pyridine and ester group (counterions removed for clarity); F, planes of stacked aromatic rings shown with centroids of stacked rings and plane inclinations indicated. Hydrogen bond parameters: C–O distances (Å), C–H–O distances (Å), C–H–O angles (deg) A: 3.291, 2.560, 133.96; B: 3.818, 3.116, 129.64; C: 3.284, 2.339, 161.30; D: 3.403, 2.783, 121.72; E: 3.601, 2.826, 136.44; F: 3.264, 2.332, 156.38; G: 3.370, 2.828, 115.61; H: 3.866, 3.024, 144.66; I: 3.004, 2.327, 127.76; J: 3.140, 2.607, 115.86; K: 3.275, 2.426, 148.72; L: 3.248, 2.692, 117.95; M: 3.435, 3.066, 104.95. Face-to-face π-stacking parameters: centroid-centroid distance (Å): N) 3.586; O) 3.782; ring plane/ring plane inclinations (deg): (i) 7.68°; (ii) 1.63°

3 Å in spacing. The second methyl group of the complex sits directly outside the cryptand's cavity and is hydrogen-bonded to the oxygen of the TFSI counterion. In total, the highly dispersed negative charge over the TFSI counterion and multiple oxygen atoms allow for the anion to play a greater role in interacting with the paraquat cation via hydrogen bonding. The result is a complex that contains more and stronger hydrogen bonds, leading to a higher association constant.

Switching to the TFSI counterion offers a near doubling of the association constant for **6•8** ($K_a = 2.22 \times 10^6$) relative to **6•7**. The complex of **6** with the benzyl paraquat **11** gave a slight decrease in binding relative to **6•7**, with lower ΔH and ΔS. Surprisingly, the association constant for **6•11** in DCM at 25°C, 1.41×10^6 mol L^{-1}, was less than the complex of **6•8** in acetone at 25°C, 2.22×10^6 mol L^{-1}; this may reflect solvation energies of the components in some manner.

Encouraged by the results for **5•11** in DCM, we speculated that the benzyl group of **11** could be used to further increase the association constant with a cryptand that also contained a benzyl group, because there would be an increased opportunity for π-stacking. To test this hypothesis, new cryptand **18** was prepared as shown in Scheme 1; the use of the diisopropyl ester in the alkylation step essentially prevented N-alkylation via steric constraints, whereas the diethyl ester produced a lower yield of **15**, which was contaminated with ~20% of N-alkylated product. The formation of **18** by a new templation method now results in a 74% yield.[14]

An ITC study (Figure 3) proved part of the hypothesis correct; a fivefold increase in the association constant was observed for **18•11** ($K_a = 5.35 \times 10^6$ mol L^{-1}) compared to **5•11**. The belief that this would be driven by π-stacking, however, was possibly incorrect. Figure 4 shows the crystal structure of **18•11**. Unfortunately, only two of the four crystallographically unique TFSI anions could be located. The remaining two TFSI anions are in a channel and are too heavily disordered to locate the individual atoms. Although this affects the overall quality of the structure and thus the uncertainties in both lengths and angles, the hosts and guests are clearly identified in the structure and provide useful information about the binding interactions. The 4-bromobenzyl rings link two adjacent cryptands via interaction of their 2 protons

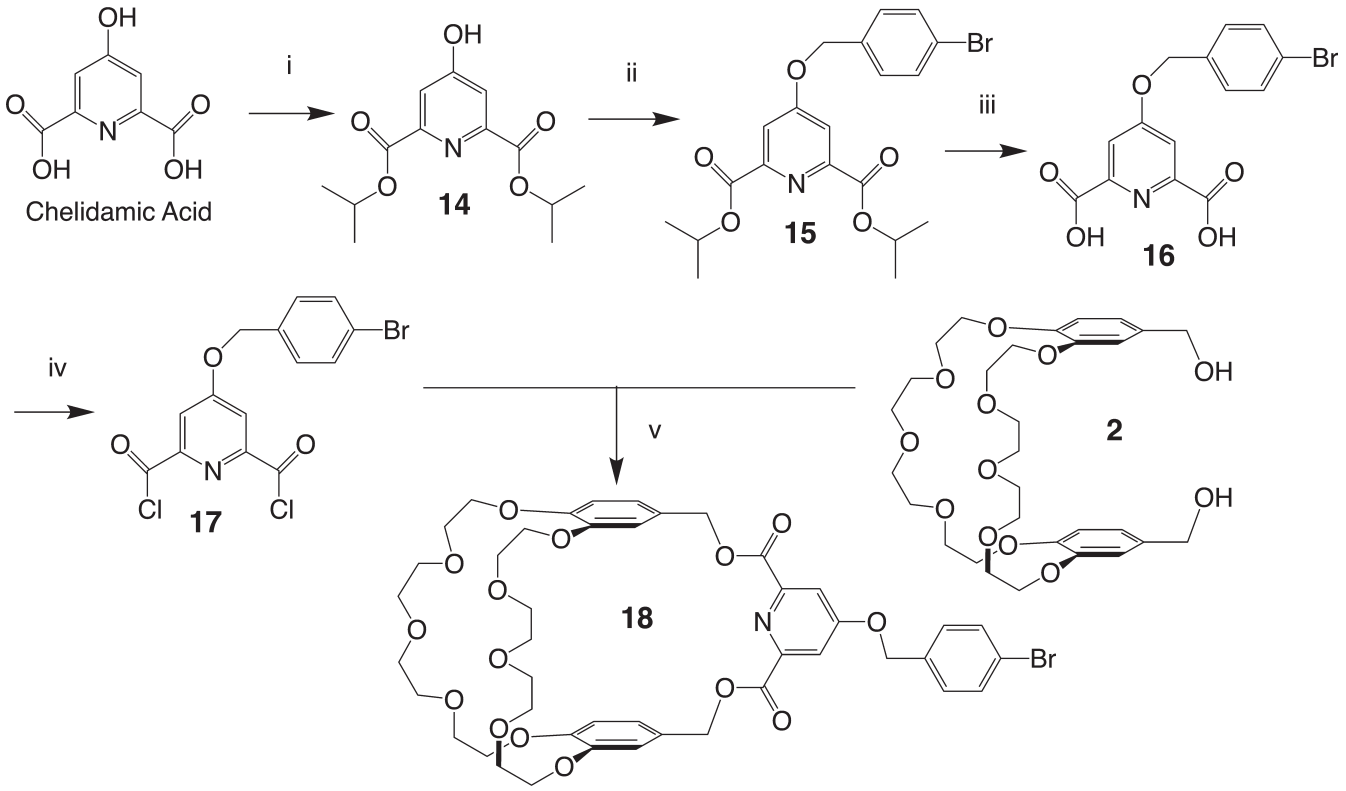

SCHEME 1 Synthesis of new cryptand **18**: (i) iPrOH/H_2SO_4 reflux 36 h, 86%; (ii) *p*-$BrC_6H_4CH_2Br/K_2CO_3$/acetone, reflux 8 h, 87%; (iii) KOH/H_2O/THF, rt, 12 h, 99%; (iv) $SOCl_2$/cat. DMF, reflux 4 h, 100%; (v) DCM pseudo-high dilution via syringe pump addition, then 3 days at rt, 46%

with ether oxygen atoms of the cryptands; in Figure 4b, the hydrogen bonds labeled A and B have bond distances H–O (C–H–O angles) of 2.532 (154.80°) and 2.855 (158.91°), respectively.

The increase in association constant for **18•11** may be partly attributed to the substituent affect on the basicity of the pyridyl nitrogen atom. Unique to **18•11** over **5•11** is the interaction of TFSI with the host: in Figure 4c two bonds (C and D) at 2.717 and 3.020 Å. The other two oxygen atoms of TFSI hydrogen bond to the paraquat, I, J, F, and G in Figure 4d. In regard to the electron releasing effect of the 4-bromobenzyloxy group, it can be seen in Figure 4g that the nitrogen-hydrogen bonds U and V (3.092 and 2.276 Å, respectively) are strong when compared to the nitrogen-hydrogen bond lengths of M and L (3.066 and 2.692 Å, respectively) found in **5•8** (Figure 2e).

It was anticipated that the electron-deficient pentafluorophenyl rings of **13** could greatly increase the acidity of the benzylic protons and thereby ultimately drive the binding constant higher with cryptand **5**. In the ^{1}H NMR spectrum, the benzylic protons of **13** appear 0.25 ppm downfield from those of hydrogenated analog **11**, indicating deshielding and more acidic protons. However, by changing to fluorinated rings, solubility in DCM was lost. From Table 4, it can be

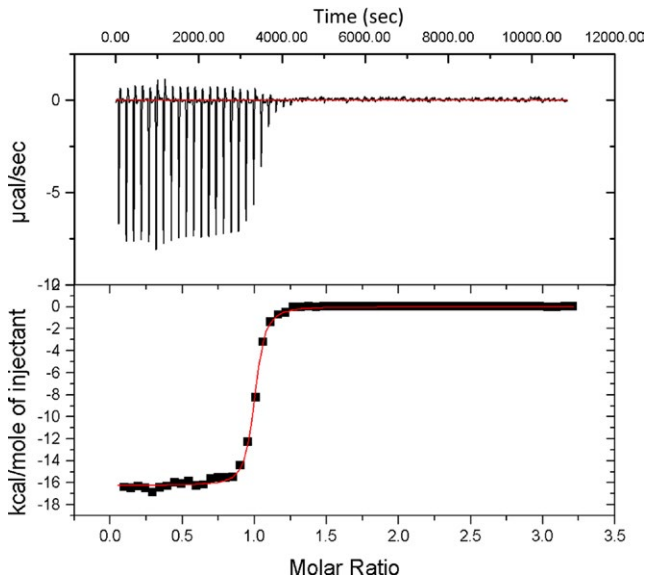

FIGURE 3 ITC titration of **11** into **18** in DCM at 25°C: $K_a = 5.35\ (\pm 0.36) \times 10^6\ M^{-1}$, $\Delta\Gamma = -9.17\ (\pm 0.04)$ kcal/mol, $\Delta H = -16.3\ (\pm 0.6)$ kcal/mol, $\Delta S = -23.9\ (\pm 2.2)$ cal/mol·deg

seen that despite the benzylic protons in **13** being more acidic, the binding constant decreased by an order of magnitude compared to **11**; ΔH decreased markedly from −18.1

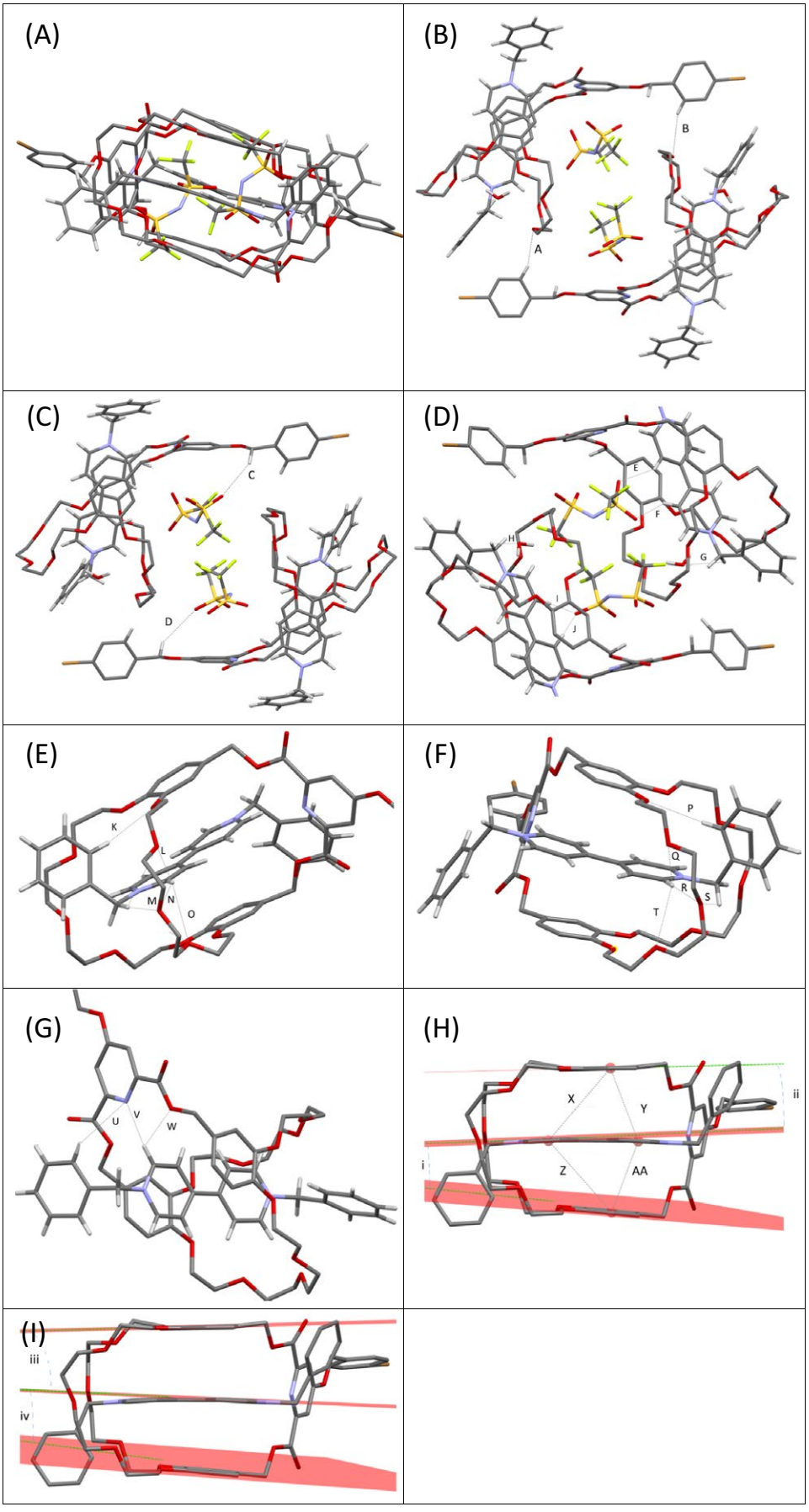
(A)
(B)
A
B
(C)
C
D
(D)
E
F
G
H
I
J
(E)
K
L
M
N
O
(F)
P
Q
R
S
T
(G)
U
V
W
(H)
X
Y
Z
AA
i
ii
(I)
iii
iv

FIGURE 4 Incomplete crystal structure of **18•11** grown by liquid-liquid diffusion of pentane into a 1:1 v:v mixture of dichloromethane:acetone; hydrogens which are not hydrogen-bonded removed for clarity; A, side view; B, top view with cryptand-cryptand hydrogen bonding; C, TFSI hydrogen bonding to cryptand; D, TFSI and water hydrogen bonding to paraquat; E, hydrogen bonding with *m*-ethyleneoxy chain; F, hydrogen bonding with *p*-ethyleneoxy chain; G, hydrogen bonding at the pyridyl arm; hydrogen bond parameters: C–O distances (Å), C–H–O distances (Å), C–H–O angles (deg) A: 3.417, 2.532, 154.80; B: 3.758, 2.855, 158.91; C: 3.566, 2.717, 144.13; D: 3.793, 3.020, 135.71; E: 3.260, 2.428, 146.08; F: 3.414, 2.616, 141.89; G: 3.149, 2.745, 104.97; H: 3.295, 2.597, 127.53; I: 3.418, 2.515, 158.62; J: 3.368, 2.467, 158.21; K: 3.430, 2.529, 158.30; L: 3.104, 2.469, 124.18; M: 3.239, 2.261, 169.92; N: 3.502, 2.693, 143.32; O: 3.145, 2.803, 102.23; P: 3.493, 2.745, 136.13; Q: 3.110, 2.573, 115.97; R: 3.141, 2.208, 166.30; S: 3.554, 3.050, 112.89; T: 3.300, 2.833, 111.26; U: 3.790, 3.092, 131.53; V: 3.183, 2.276, 159.36; W: 3.059, 2.496, 117.87. Face-to-face π-stacking parameters: centroid-centroid distance (Å): X: 4.501; Y: 3.696; Z: 4.497; AA: 3.713; ring plane/ring plane inclinations (deg): (i) 7.90°; (ii) 1.10°; (iii) 3.97°; (iv) 3.65°

to −12.9 kcal/mol, even though ΔS also decreased substantially. Thus, the anticipated increased acidity of the benzylic protons of **13** did not result in improved complexation.

Interestingly, a linear correlation was found between entropy and enthalpy values (Figure 5). This type of correlation has been observed and described in the literature in terms of enthalpy-entropy compensation.[20–22] Correlations such as these have recently driven arguments for a connection between entropy and internally stored energies,[23] hidden term(s) connecting enthalpy and entropy,[24] and the potential for a fourth law of thermodynamics that explains intermolecular binding processes.[20]

3 | CONCLUSIONS

In conclusion, the alteration of the dimethyl paraquat PF_6 motif (**7**) to a dibenzyl paraquat TFSI motif (**11**) resulted in increased solubility of the paraquat salt in less polar solvents. In the less polar solvent DCM, the association constant of dibenzo-30-crown-10-based pyridyl cryptand **5** with dibenzyl paraquat TFSI (**11**) increased by an order of magnitude over the analogous dimethyl paraquat PF_6 (**7**) complex in acetone. However, the association constant of the 32-crown-10-based cryptand **6** did not increase similarly; the K_a of **6** with **11** in DCM actually decreased slightly compared to dimethyl paraquat PF_6 (**7**) in acetone. Although cryptand **6** benefited from the change of PF_6 to TFSI with dimethyl paraquat (**7** vs **8**), at best only a doubling in K_a was observed. Inspection of several paraquat cryptand combinations (**7** vs **8**, **10** vs **11**) revealed that TFSI-containing paraquats generally yielded higher association constants than their PF_6 counterparts, but gains were modest. A dibenzo-30-crown-10-based pyridyl cryptand containing a *p*-bromobenzyloxy group in the pyridyl ring (**18**) led to $K_a = 5.35 \times 10^6$ mol L^{-1} with dibenzyl paraquat TFSI (**11**).

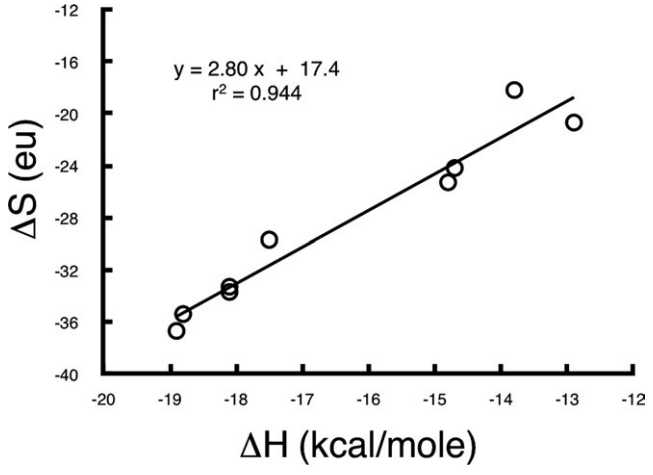

FIGURE 5 Plot of entropies vs enthalpies for complexation of cryptands **5** and **6** with paraquats **7**, **8**, **10**, **11**, and **13**; values in acetone or DCM from Table 4

4 | EXPERIMENTAL

4.1 | Measurements

^{1}H NMR spectra were obtained on JEOL ECLIPSE-500, BRUKER-500, and AGILENT-NMR-vnmrs400 spectrometers; ^{13}C NMR spectra were collected at 125, 125, and 101 MHz, respectively, on these instruments. HR-MS were obtained using an Agilent LC-ESI-TOF system with acetonitrile as solvent. Reagents were purchased and used as received without further purification unless otherwise stated. Compounds **2**,[6] **5**,[6] **6**,[7] **7**,[25] **10**,[26] and **13**[27] were prepared as described by the literature procedures; similar yields were achieved. Crystals of **5•8** were grown from an equimolar solution of chloroform:acetone 1:1 (v:v) by liquid-liquid diffusion of diethyl ether. Crystals of **18•11** were grown from an equimolar DCM:acetone 1:1 (v:v) solution by liquid-liquid diffusion of pentane.

4.2 | Solubility testing

A mixture of solvent and excess paraquat salt was made and placed in a water bath at 25°C for 8 hour. A 5.00 mL of aliquot was removed from the saturated solution using a volumetric pipette and placed in a clean, tared vial. Solvent removal and determination of the mass of the solid residue allowed calculation of the concentration of the saturated solution.

4.3 | Sample ITC titration

The following is an example using **5•11** in DCM at 25°C. Host **5** was loaded into the cell of the instrument at a concentration of 0.160 mmol L^{-1}, while a 250-μL ITC syringe was

loaded with **11** at a concentration of 2.291 mmol L^{-1}. The instrument was set to high gain (high sensitivity). The titration was achieved through 60 injections of 4.167 µL every 180 seconds; a primary filter period of 1 second and a secondary filter period of 3 second were applied (filter period switch time 60 seconds). A background titration used exactly the same titration conditions with the exception that the solution of **5** in the cell was replaced with pure DCM. The heats for the dilution experiment were subtracted from the heats for the titration of **11** with **5**. Analysis of the data was carried out using software provided by the manufacturer; the first datum point was ignored. A "One Set of Sites" model was used; stoichiometries other than 1:1 provided unsatisfactory fits.

4.4 | Dimethyl paraquat TFSI (8)

Dimethyl paraquat diiodide[28] (2.65 g, 6.02 mmol) in 20 mL of water was added to a solution of LiTFSI (4.10 g, 15.6 mmol) in 10 mL of water. The resulting precipitate was filtered and allowed to air-dry to provide a colorless solid: 4.32 g (96%), recrystallized from water and acetone three times, 2.88 g (64%), mp 125.9-127.9°C; lit. mp 130°C.[29] ^{1}H NMR (500 MHz, acetone-d_6) δ 9.42 (s, 4H), 8.87 (s, 4H), 4.77 (s, 6H). ^{13}C NMR (126 MHz, acetone-d_6) δ 150.67 (s), 147.88 (s), 127.76 (s), 120.95 (q, J = 322 Hz), 49.46 (s) (5 signals expected and 5 signals found). High res ESI MS: calc. for $C_{16}H_{14}NaN_4O_8S_4F_{12}$ $[M + Na]^+$: m/z 768.9395; found: m/z 768.9405 (error 1.3 ppm).

4.5 | Dimethyl paraquat TPFB (9)

Dimethyl paraquat diiodide[28] (63.1 mg, 0.143 mmol) in 3 mL of water was added to a solution of lithium tetrakis(pentafluorophenyl)borate tri(ethyl etherate) (310.4 mg, 0.3417 mmol) in 3 mL of water. The resulting precipitate was filtered and allowed to air-dry to provide a colorless solid: 0.2171 g (98%), mp 204.6-208.5°C. ^{1}H NMR (400 MHz, acetone-d_6) δ 9.51 (d, J = 7 Hz, 4H), 8.96 (d, J = 7 Hz, 4H), 4.79 (s, 6H). ^{13}C NMR (101 MHz, acetone-d_6) δ 149.81 (s), 147.08 (s, overlap), 148.13 (br d, J = 237 Hz, overlap), 143.13 (br d, J = 773 Hz, overlap), 136.11 (br d, J = 253 Hz), 136.90 (s, overlap), 126.90 (s), 48.64 (s) (8 signals expected and 8 signals found). High res ESI MS: calc. for $C_{36}H_{14}F_{20}N_2B$ $[M - TPFB]^+$: m/z 865.0925; found: m/z 865.0890 (error 4.0 ppm).

4.6 | General procedure 1: dibenzyl paraquat TFSI (11)

To a round bottom flask containing acetonitrile (100 mL) were added 4,4′-dipyridyl (2.03 g, 13.0 mmol) and benzyl bromide (5.0 mL, 42 mmol) under nitrogen. The reaction mixture was held at reflux for 21 hours, after which the solvent was removed by rotary evaporation. The crude material was triturated with acetonitrile and DCM, followed by collection on a fritted glass filter where it was washed with DCM and air-dried: 6.45 g (99%), mp 260 (dec); lit. mp 260 (dec).[30] The precipitate (1.47 g, 2.95 mmol) in 10 mL of water was mixed with a solution of LiTFSI (2.11 g, 8.02 mmol) in 5 mL of water. The precipitate was filtered, washed with water, and allowed to air-dry; this provided a colorless solid: 2.6514 g (100%), recrystallized from water-acetone mixture (×3), mp 112.4-113.3°C. ^{1}H NMR (500 MHz, DMSO-d_6) δ 9.52 (d, J = 7 Hz, 4H), 8.75 (d, J = 7 Hz, 4H), 7.62 (d, J = 7 Hz, 4H), 7.52-7.41 (m, 6H), 5.96 (s, 4H). ^{13}C NMR (126 MHz, DMSO-d_6) δ 149.34 (s), 145.65 (s), 134.01 (s), 129.48 (s), 129.22 (s), 128.86 (s), 127.23 (s), 119.45 (q, J = 323 Hz), 63.54 (s) (9 peaks expected and 9 peaks found). High res ESI MS: calc. for $C_{28}H_{26}F_{12}N_5O_8S_4$ $[M + NH_4]^+$: m/z 916.0467; found: m/z 916.0503 (error 3.9 ppm).

4.7 | Dibenzyl paraquat TPPB (12)

General procedure 1 was used to produce an off-white solid, 162.3 mg (98%), mp 240.6-242.3°C, using dibenzyl paraquat dibromide (48.6 mg, 0.0975 mmol) and lithium tetrakis(pentafluorophenyl)borate tri(ethyl etherate) (286.0 mg, 0.3148 mmol) dissolved in 3 mL of water. ^{1}H NMR (400 MHz, acetone-d_6) δ 9.63 (d, J = 7 Hz, 4H), 8.96 (d, J = 7 Hz, 4H), 7.75-7.58 (m, 4H), 7.57-7.43 (m, 6H), 6.22 (s, 4H). ^{13}C NMR (101 MHz, acetone-d_6) δ 150.67 (s), 148.15 (br d, J = 245 Hz), 146.09 (s, overlap), 142.71 (br d, J = 683 Hz), 136.10 (br d, J = 254 Hz), 136.92 (s, overlap), 133.24 (s), 130.05 (s), 129.58 (s), 129.17 (s), 127.77 (s), 64.98 (s) (12 signals expected and 12 signals found). High res ESI MS: calc. for $C_{72}H_{22}F_{40}NaN_2B_2$ $[M + Na]^+$: m/z 1719.1223; found: m/z 1719.1303 (error 4.7 ppm).

4.8 | *N*,*N*′-Bis[pentafluorobenzyl]-4,4′-bipyridinium TFSI (13)

To a round bottom flask containing acetonitrile (20 mL) were added 4,4′-dipyridyl (0.7161 g, 4.585 mmol) and 2,3,4,5,6-pentafluorobenzyl bromide (2.0 mL, 13 mmol) under nitrogen. The reaction mixture was held at reflux for 21 hours, after which the solvent was removed by rotary evaporation. The crude material was triturated with acetonitrile and DCM, followed by collection on a fritted glass filter where it was washed with DCM and air-dried. The solid was dissolved in 5 mL of water and mixed with a solution of LiTFSI (3.29 g, 11.5 mmol) in 5 mL of water. The precipitate was filtered, washed with water, and allowed to air-dry: a colorless solid, 4.88 g (99%), mp 166.5-167.9°C. ^{1}H NMR (500 MHz, DMSO-d_6) δ 9.38 (d, J = 7 Hz, 4H), 8.75 (d, J = 7 Hz, 4H), 6.21 (s, 4H). ^{13}C NMR (126 MHz, DMSO-d_6)

δ 150.13 (s), 146.70 (s), 146.09 (br d, $J = 255$ Hz), 142.25 (br d, $J = 255$ Hz), 137.71 (dt, $J = 252$, 13 Hz), 127.66 (s), 119.9 (q, J = 323 Hz), 107.87 (tt, $J = 8$, 4 Hz), 51.99 (s) (9 signals expected and 9 signals found). High res MS: calc. for $C_{24}H_{13}F_{10}N_2$ $[M - 2TFSI + H]^+$: *m/z* 260.0493; found: *m/z* 260.0492 (error 0.4 ppm).

4.9 | Isopropyl chelidamate (14)

A solution of isopropanol (200 mL, 2.61 mol), sulfuric acid (0.20 mL, 3.8 mmol), and chelidamic acid[27] (2.48 g, 13.5 mmol) was held at reflux under nitrogen for 36 hours. Solvent was removed by rotary evaporation, and the crude material was dissolved in chloroform, washed with 5% Na_2CO_3 (×1), 2% $NaHCO_3$ (×4), water (×2), saturated NaCl (×1), and dried over sodium sulfate. Filtration and removal of the solvent provided the desired product as a colorless solid: 3.11 g (86%), mp 128.7-129.8°C; lit. mp 145-146°C.[31] ^{1}H NMR (500 MHz, $CDCl_3$) δ 7.11 (s, 2H), 5.33-5.24 (m, 2H), 1.40 (d, $J = 6$ Hz, 12H). ^{13}C NMR (126 MHz, $CDCl_3$) δ 181.06 (s), 161.07 (s), 136.91 (s), 120.55 (s), 72.05 (s), 21.73 (s) (6 peaks expected and 6 peaks found). HR-MS: calc. for $C_{13}H_{18}O_5N$ $[M + H]^+$: *m/z* 268.1179; found: *m/z* 268.1193 (error 5.2 ppm).

4.10 | Diisopropyl 4-(*p*-bromobenzyloxy) pyridine-2,6-dicarboxylate (15)

A mixture of acetone (125 mL), isopropyl chelidamate (**14**, 4.30 g, 16.1 mmol), *p*-bromobenzyl bromide (4.54 g, 18.2 mmol), and potassium carbonate (3.59 g, 26.0 mmol) was held at reflux under nitrogen for 8 hours, filtered through Celite p545®, and the solvent was removed by rotary evaporation. The crude material was triturated with hexanes, and the product was collected as a colorless solid: 6.14 g (87%), mp 123.5-124.6°C. ^{1}H NMR (500 MHz, $CDCl_3$) δ 7.80 (s, 2H), 7.55 (d, $J = 8$ Hz, 2H), 7.32 (d, $J = 8$ Hz, 2H), 5.29 (hept, $J = 6$ Hz, 2H), 5.17 (s, 2H), 1.43 (d, $J = 6$ Hz, 12H). ^{13}C NMR (126 MHz, $CDCl_3$) δ 166.23 (s), 164.06 (s), 150.72 (s), 133.84 (s), 132.04 (s), 129.36 (s), 122.80 (s), 114.27 (s), 70.23 (s), 69.91 (s), 21.81 (s) (11 peaks expected and 11 peaks found); HR ESI MS: calc. for $C_{20}H_{23}O_5NBr$ $[M + H]^+$: *m/z* 436.0754; found: *m/z* 436.0760 (error 1 ppm).

4.11 | 4-(*p*-Bromobenzyloxy)pyridine-2,6-dicarboxylic acid (16)

A solution of diisopropyl 4-(*p*-bromobenzyloxy)pyridine-2,6-dicarboxylate (**15**, 2.65 g, 6.07 mmol), 10% wt. KOH (50 mL), and THF (50 mL) was stirred for 12 hour at room temperature. THF was removed by rotary evaporation. The remaining aqueous solution was carefully acidified to pH 1, chilled, and filtered to produce a colorless solid, 2.13 g (99%), mp 185.7-187.7°C. ^{1}H NMR (400 MHz, DMSO-d_6) δ 7.80 (s, 2H), 7.62 (s, 2H), 7.46 (d, $J = 8$ Hz, 2H), 5.36 (s, 2H). ^{13}C NMR (101 MHz, DMSO-d_6) δ 163.17 (s), 162.12 (s), 146.66 (s), 131.94 (s), 128.36 (s), 126.81 (s), 118.32 (s), 110.75 (s), 66.17 (s) (9 peaks expected and 9 peaks found). HR ESI MS: calc. for $C_{14}H_{11}O_5NBr$ $[M + H]^+$: *m/z* 351.9815; found: *m/z* 351.9827 (error 3.4 ppm).

4.12 | 4-(*p*-Bromobenzyloxy)pyridine-2,6-dicarboxylic acid chloride (17)

4-(*p*-Bromobenzyloxy)pyridine-2,6-dicarboxylic acid (**16**, 0.5177 g, 1.470 mmol), thionyl chloride (5 mL, 0.07 mol) and DMF (1 drop) were held at reflux for 4 hours with magnetic stirring. Excess thionyl chloride was removed by distillation to provide 0.5719 g (100%) of an off-white solid with a yellow tint, which was used directly without characterization.

4.13 | Dibenzo-30-crown-10-based 4-(*p*-bromobenzyloxy)pyridyl cryptand (18)

cis-Dibenzo-30-crown-10 diol[6] (**2**, 0.72256 g, 1.211 mmol) and 4-(*p*-bromobenzyloxy)pyridine-2,6-dicarboxylic acid chloride (**17**, 0.4719 g, 1.213 mmol) were freshly prepared and dissolved separately in 50.0 mL of freshly distilled DCM. The two solutions were loaded into plastic syringes with HPLC tubing sealed to the syringe. Additions from the syringes were made to a stirred solution of pyridine (3.0 mL, 37 mmol) in DCM (2.7 L, freshly distilled) via syringe pump at 1.5 mL/h. After additions were complete, the reaction mixture was allowed to stir for 3 days, after which time solvent was removed by rotary evaporation, and the resulting solid was dissolved in chloroform. The crude mixture was washed with 1 mol L^{-1} HCl (×1) and water (×3). Solvent was removed by rotary evaporation. The resulting residue was purified by column chromatography using neutral alumina, eluting with chloroform:methanol (99:1); 0.5082 g (46%) of colorless solid, mp 188.8-192.7°C. ^{1}H NMR (400 MHz, $CDCl_3$) δ 7.88 (s, 2H), 7.55 (d, $J = 8$ Hz, 2H), 7.32 (d, $J = 8$ Hz, 2H), 6.94-6.92 (m, 4H), 6.77 (d, $J = 9$ Hz, 2H), 5.30 (s, 4H), 5.18 (s, 2H), 4.20-4.11 (m, 4H), 4.03-3.97 (m, 4H), 3.95-3.90 (m, 4H), 3.84-3.78 (m, 4H), 3.74 (m, 4H), 3.72-3.67 (m, 8H), 3.64 (m, 4H). ^{13}C NMR (126 MHz, $CDCl_3$) δ 166.43 (s), 164.88 (s), 150.24 (s), 149.12 (s), 149.00 (s), 133.85 (s), 132.14 (s), 129.37 (s), 128.19 (s), 122.87 (s), 121.80 (s), 114.80 (s), 114.34 (s), 114.02 (s), 71.10 (s), 70.86 (s), 70.83 (s), 70.73 (s), 70.03 (s), 69.79 (s), 69.55 (s), 69.09 (s), 68.90 (s), 67.83 (s) (24 peaks expected and 24 peaks found). High res ESI MS: calc. for $C_{44}H_{51}NO_{15}Br$ $[M + H]^{+1}$: *m/z* 912.2437; found: *m/z* 912.2452 (error 1.6 ppm).

ACKNOWLEDGMENTS

We acknowledge and are thankful for support from the National Science Foundation (DMR 0704076, CHE-1106899, CHE-1507553).

ORCID

Harry W. Gibson http://orcid.org/0000-0001-9178-6691

REFERENCES

[1] a) L. Brunsveld, B. J. B. Folmer, E. W. Meijer, R. P. Sijbesma, *Chem. Rev.* **2001**, *101*, p. 4071; b) F. Huang, D. S. Nagvekar, X. Zhou, H. W. Gibson, *Macromolecules* **2007**, *40*, 3561.
[2] C. He, Z. Shi, Q. Zhou, S. Li, N. Li, F. Huang, *J. Org. Chem.* **2008**, *73*, 5872.
[3] B. L. Allwood, H. Shahriari-Zavareh, J. F. Stoddart, D. J. Williams, *J. Chem. Soc. Chem. Comm.* **1987**, 1058.
[4] a) Z. Niu, C. Slebodnick, D. Schoonover, H. Azurmendi, K. Harich, H. W. Gibson, *Org. Lett.* **2011**, *13*, 3992. b) W. S. Bryant, J. W. Jones, P. E. Mason, I. Guzei, A. L. Rheingold, F. R. Fronczek, D. S. Nagvekar, H. W. Gibson, *Org. Lett.* **1999**, *1*, 1001.
[5] P. R. Ashton, D. Philp, M. V. Reddington, A. M. Z. Slawin, N. Spencer, J. F. Stoddart, D. J. Williams, *J. Chem. Soc. Chem. Comm.* **1991**, 1680.
[6] A. M. P. Pederson, E. M. Ward, D. V. Schoonover, C. Slebodnick, H. W. Gibson, *J. Org. Chem.* **2008**, *73*, 9094.
[7] F. Huang, K. A. Switek, L. N. Zakharov, F. R. Fronczek, C. Slebodnick, M. Lam, J. A. Golen, W. S. Bryant, P. E. Mason, A. L. Rheingold, M. Ashraf-Khorassani, H. W. Gibson, *J. Org. Chem.* **2005**, *70*, 3231.
[8] A. M. P. Pederson, R. C. Vetor, M. A. Rouser, F. Huang, C. Slebodnick, D. V. Schoonover, H. W. Gibson, *J. Org. Chem.* **2008**, *73*, 5570.
[9] F. Huang, H. W. Gibson, W. S. Bryant, D. S. Nagvekar, F. R. Fronczek, *J. Am. Chem. Soc.* **2003**, *125*, 9367.
[10] M. Zhang, X. Yan, F. Huang, Z. Niu, H. W. Gibson, *Acc. Chem. Res.* **2014**, *47*, 1995.
[11] A. M.-P. Pederson, T. L. Price Jr., C. Slebodnick, D. V. Schoonover, H. W. Gibson, *J. Org. Chem.* **2017**, *82*, 8489.
[12] H. R. Wessels, H. W. Gibson, *Tetrahedron* **2016**, *72*, 396.
[13] H. W. Gibson, H. Wang, K. Bonrad, J. W. Jones, C. Slebodnick, B. Habenicht, P. Lobue, *Org. Biomol. Chem.* **2005**, *3*, 2114.
[14] T. L. Price Jr., H. R. Wessels, C. Slebodnick, H. W. Gibson, *J. Org. Chem.* **2017**, *82*, 8117.
[15] H. W. Gibson, D. S. Nagvekar, *Can. J. Chem.* **1997**, *75*, 1375.
[16] T. L. Greaves, C. J. Drummond, *Chem. Soc. Rev.* **2013**, *42*, 1096.
[17] T. L. Greaves, C. J. Drummond, *Chem. Rev.* **2015**, *115*, 11379.
[18] H. W. Gibson, H. Wang, C. Slebodnick, J. Merola, W. S. Kassel, A. L. Rheingold, *J. Org. Chem.* **2007**, *72*, 3381.
[19] X. Yan, P. Wei, M. Zhang, X. Chi, J. Liu, F. Huang, *Org. Lett.* **2011**, *13*, 6370.
[20] C. Piguet, *Dalton Trans.* **2011**, *40*, 8059.
[21] P. Gilli, V. Ferretti, G. Gilli, P. A. Borea, *J. Phys. Chem.* **1994**, *98*, 1515.
[22] A. Pan, T. Biswas, A. K. Rakshit, S. P. Moulik, *J. Phys. Chem. B* **2015**, *119*, 15876.
[23] F. L. Lambert, H. S. Leff, *J. Chem. Educ.* **2009**, *86*, p. 94.
[24] E. B. Starikov, B. Nordén, *Chem. Phys. Lett.* **2012**, *538*, 118.
[25] B. Tang, H.-M. Yang, W.-J. Hu, M.-L. Ma, Y. A. Liu, J.-S. Li, B. Jiang, K. Wen, *Eur. J. Org. Chem.* **2014**, *2014*, 6925.
[26] J.-F. Xu, Z. Huang, L. Chen, B. Qin, Q. Song, Z. Wang, X. Zhang, *ACS Macro Lett.* **2015**, *4*, 1410.
[27] G. Howáth, C. Rusa, Z. Köntös, J. Gerencsér, P. Huszthy, *Synth. Commun.* **1999**, *29*, 3719.
[28] L. Pescatori, A. Arduini, A. Pochini, A. Secchi, C. Massera, F. Ugozzoli, *Org. Biomol. Chem.* **2009**, *7*, 3698.
[29] N. Jordão, L. Cabrita, F. Pina, L. C. Branco, *Chem. Eur. J.* **2014**, *20*, 3982.
[30] M. Albrecht, M. Yulikov, T. Kohn, G. Jeschke, J. Adams, A. Schmidt, *J. Mater. Chem.* **2010**, *20*, 3025.
[31] J. B. Lamture, Z. H. Zhou, A. S. Kumar, T. G. Wensel, *Inorg. Chem.* **1995**, *34*, 864.

SUPPORTING INFORMATION

Additional Supporting Information may be found online in the supporting information tab for this article.

How to cite this article: Price TL, Slebodnick C, Gibson HW. Improved complexation of paraquats with crown ether-based pyridyl cryptands. *Heteroatom Chem*. 2017;e21406. https://doi.org/10.1002/hc.21406